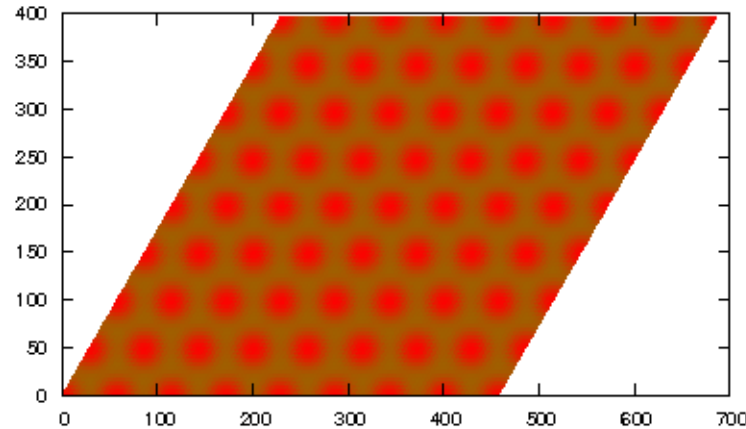


Quantum Monte Carlo Study of the Two-Dimensional Homogeneous Electron Gas



Neil D. Drummond

Department of Physics, Lancaster University

QMC and the CASINO program, TTI, Vallico Sotto, Italy

Thursday 8th August, 2013

Two-Dimensional Homogeneous Electron Gas (I)

- **2D HEG**: set of electrons moving in 2D in a uniform, inert, neutralising background.
- Hamiltonian (for finite system):

$$\hat{H} = \sum_i -\frac{1}{2}\nabla_i^2 + \sum_{j>i} v_E(\mathbf{r}_{ij}) + \frac{Nv_M}{2}.$$

Infinite-system ground-state energy per particle depends only on the **density** (specified by radius r_s of circle containing one electron on average) and **spin polarisation** [$\zeta = (N_\uparrow - N_\downarrow)/N$].

- Physical realisations:
 - *Electrons on metal surfaces*. E.g. Cu [111].
 - *Electrons on droplets of liquid He*.
 - *Inversion layers in MOS devices*. Can easily tune density. Electrons far from dopants; fewer complications due to disorder; technologically important.
 - Electrons in **2D semiconductors** (gallium chalcogenides, etc.).

Two-Dimensional Homogeneous Electron Gas (II)

- **Quantum Monte Carlo** is the most accurate first-principles method available for studying the ground-state properties of the HEG.
- We have carried out QMC studies of the 2D HEG to determine:
 1. The [zero-temperature phase diagram](#).¹
 2. The [pair-correlation function](#), [structure factor](#) and [momentum distribution](#).²
 3. The [energy band](#) and hence [quasiparticle effective mass](#).³
- Our data are of interest to
 - Experimentalists looking for ferromagnetism, Wigner crystallisation and changes to the effective mass in low-density 2D HEGs.
 - Theorists interested in constructing 2D XC functionals for DFT calculations.

¹ N. D. Drummond and R. J. Needs, Phys. Rev. Lett. **102**, 126402 (2009).

² N. D. Drummond and R. J. Needs, Phys. Rev. B **79**, 085414 (2009).

³ N. D. Drummond and R. J. Needs, Phys. Rev. B **80**, 245104 (2009).

Wigner Crystallisation in 2D (I)

- Kinetic energy dominates at high density: *form Fermi fluid to minimise it.*
- Potential energy dominates at low density: *form Wigner crystal to minimise it.*
- Wigner crystals have been observed on the surface of liquid helium⁴ and in inversion layers in MOSFET devices⁵.
- Previous QMC studies⁶ indicate that fluid–crystal transition occurs somewhere between $r_s = 25$ and 40 a.u. at zero temperature.
- Can we be more precise?

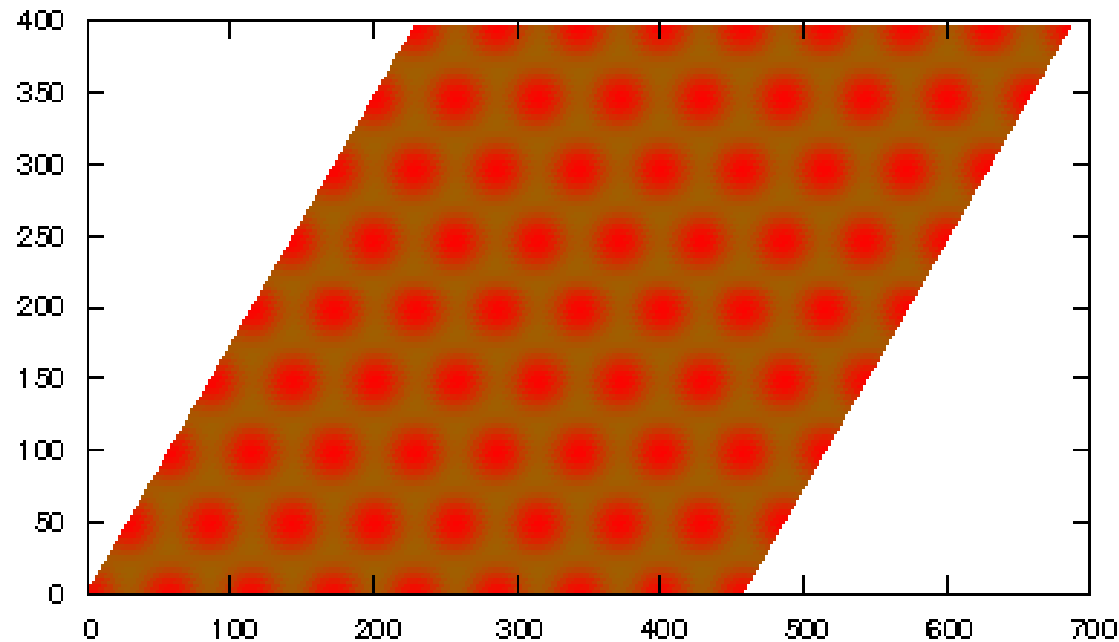
⁴ C. C. Grimes and G. Adams, Phys. Rev. Lett. **42**, 795 (1979).

⁵ E. Y. Andrei *et al.*, Phys. Rev. Lett. **60**, 2765 (1988); R. L. Willett *et al.*, Phys. Rev. B **38**, 7881 (1988).

⁶ B. Tanatar & D. M. Ceperley, Phys. Rev. B **39**, 5005 (1989); F. Rapisarda & G. Senatore, Aust. J. Phys. **49**, 161 (1996).

Wigner Crystallisation in 2D (II)

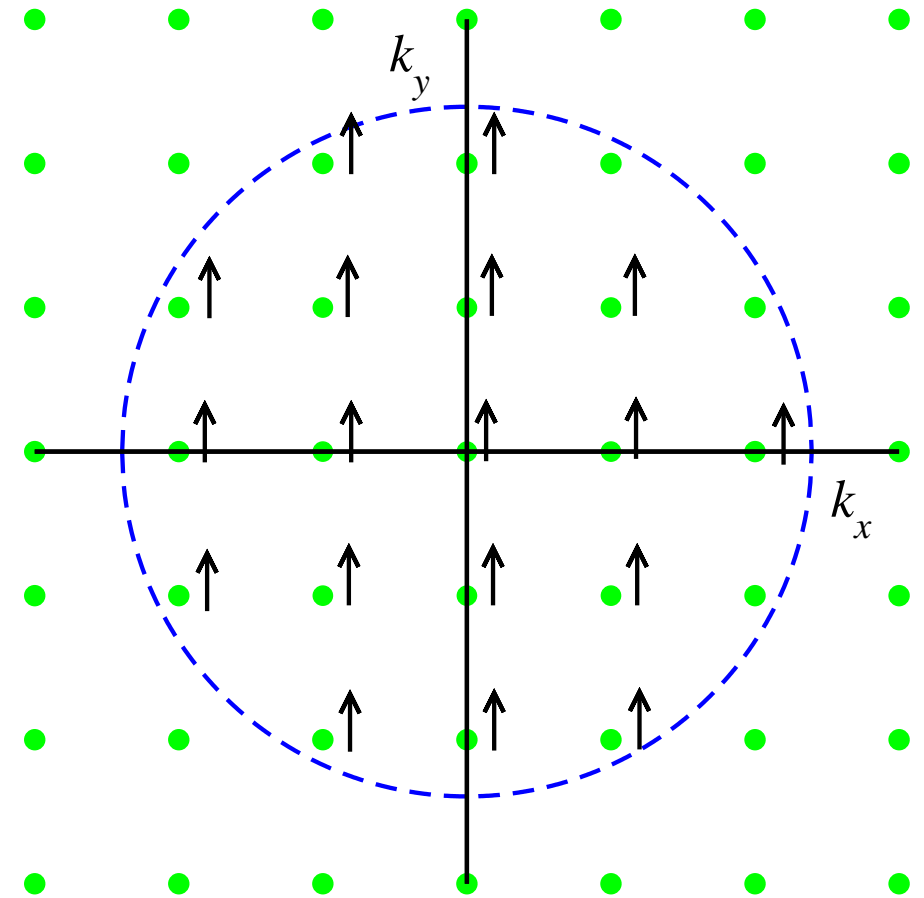
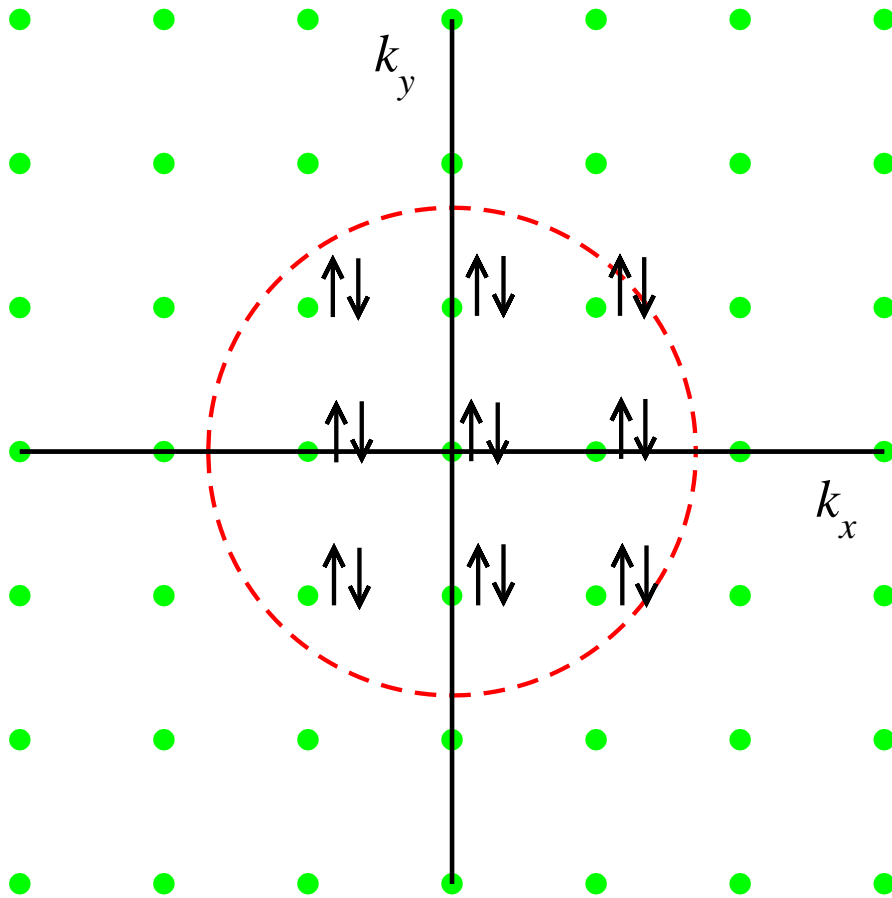
- Triangular lattice has lowest Madelung constant. Wins at low density.
- [Hartree–Fock theory](#)⁷: antiferromagnetic square lattice \rightarrow ferromagnetic triangular lattice at $r_s = 2.6$ a.u.
- We consider only triangular lattices.



⁷ J. R. Trail, M. D. Towler and R. J. Needs, Phys. Rev. B **68**, 045107 (2003).

Magnetic Behaviour of the Fermi Fluid (I)

- **Bloch transition:** paramagnetic fluid favoured at high density (doubly occupy low-momentum states to minimise KE); ferromagnetic fluid favoured at low density (keep electrons apart to minimise XC energy).



Magnetic Behaviour of the Fermi Fluid (II)

- **Hartree–Fock theory**: Bloch transition at $r_s = 2.01$ a.u. No region of stability for ferromagnetic fluid.
- **VMC**⁸: Bloch transition at $r_s = 13(2)$ a.u.; crystallisation at $r_s = 33(2)$ a.u.
- **DMC**⁹: Bloch and crystallisation transitions at $r_s = 37(5)$ a.u.
- **DMC**¹⁰: Bloch transition at $r_s = 20(2)$ a.u. and crystallisation at $r_s = 34(4)$ a.u.
- **Experiment**¹¹: “Possible evidence” of spontaneous spin polarisation at $r_s = 7.6$ a.u.
- **Open question**: is there a range of densities at which the 2D HEG forms a ferromagnetic fluid?

⁸ D. Ceperley, Phys. Rev. B **18**, 3126 (1978).

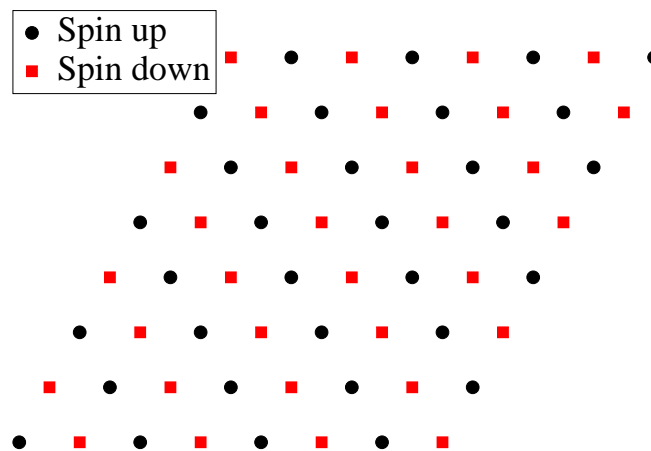
⁹ B. Tanatar and D. M. Ceperley, Phys. Rev. B **39**, 5005 (1989).

¹⁰ F. Rapisarda and G. Senatore, Aust. J. Phys. **49**, 161 (1996).

¹¹ A. Ghosh, C. J. B. Ford, M. Pepper, H. E. Beere and D. A. Ritchie, Phys. Rev. Lett. **92**, 116601 (2004).

Magnetic Behaviour of the Wigner Crystal

- Hartree-Fock theory¹²: ferromagnetic for $r_s > 2.6$ a.u.
- Multispin exchange model¹³: frustrated antiferromagnetism (spin liquid) → ferromagnetism at $r_s \leq 175(10)$ a.u.
- We have studied both ferromagnetic and antiferromagnetic triangular crystals.
- We have used striped antiferromagnetic crystals. Energy should be close to that of the spin liquid.



¹² J. R. Trail, M. D. Towler and R. J. Needs, Phys. Rev. B **68**, 045107 (2003).

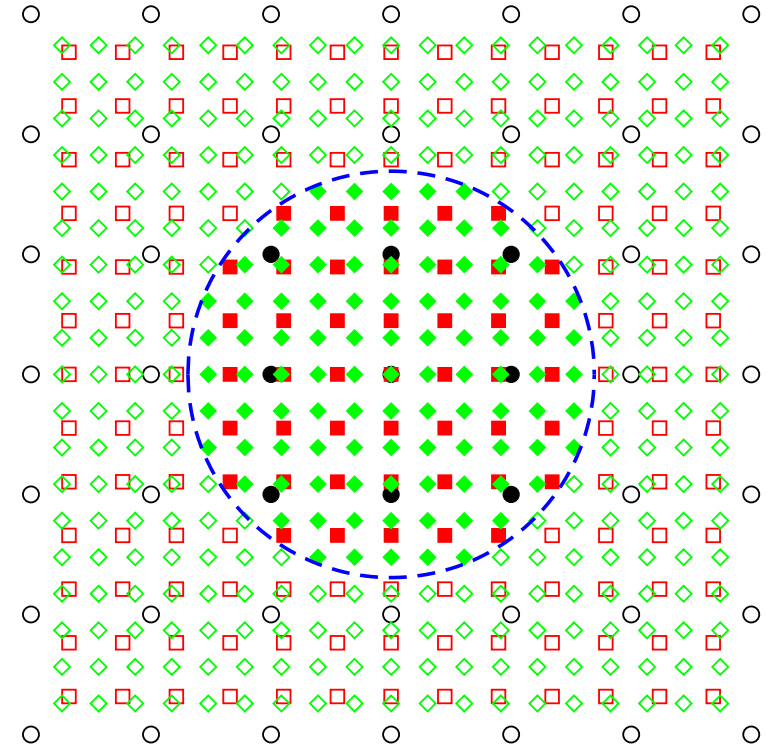
¹³ B. Bernu, L. Candido and D. M. Ceperley, Phys. Rev. Lett. **86**, 873 (2001).

Fermi Fluid: Boundary Conditions (I)

- Orbitals for Fermi fluid:

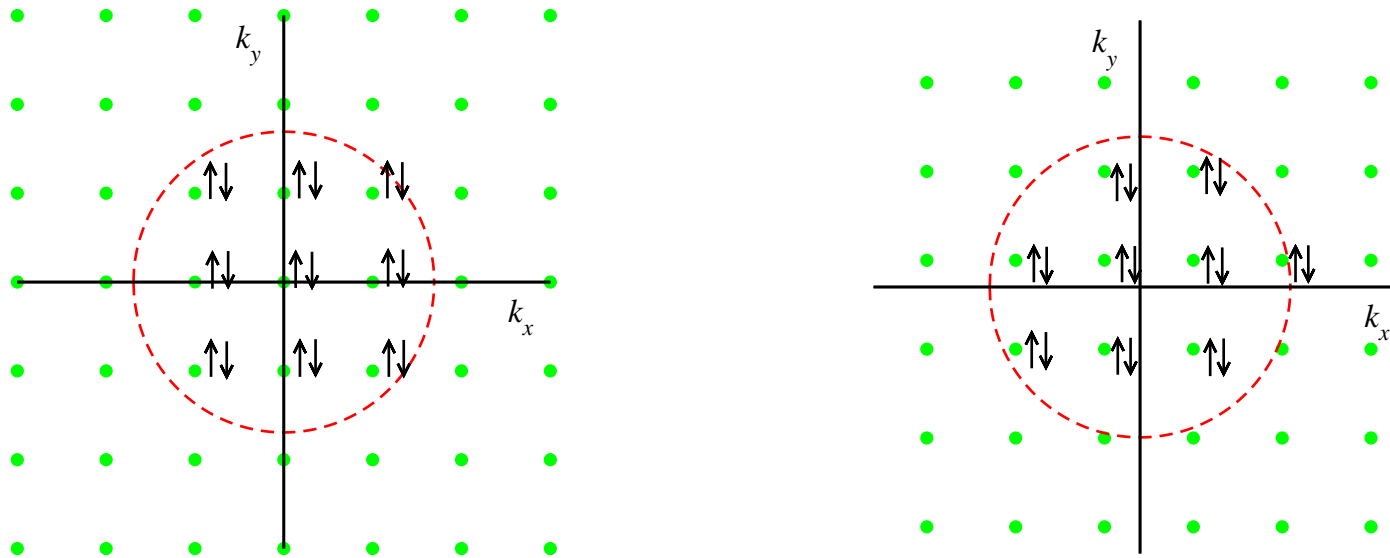
$$\phi_{\mathbf{k}}(\mathbf{r}) = \exp(i\mathbf{k} \cdot \mathbf{r}).$$

- Periodic boundary conditions on a finite cell: $\{\mathbf{k}\}$ are simulation-cell \mathbf{G} -vectors.
- Single-particle finite-size effects*: Increase N at fixed density; grid of \mathbf{G} -vectors gets finer; energy per electron jumps as shells of \mathbf{G} vectors get occupied.



Fermi Fluid: Boundary Conditions (II)

- **Twisted boundary conditions:** \mathbf{k} are simulation-cell \mathbf{G} vectors offset by $\mathbf{k}_s \in 1\text{st}$ Brillouin zone of simulation cell.



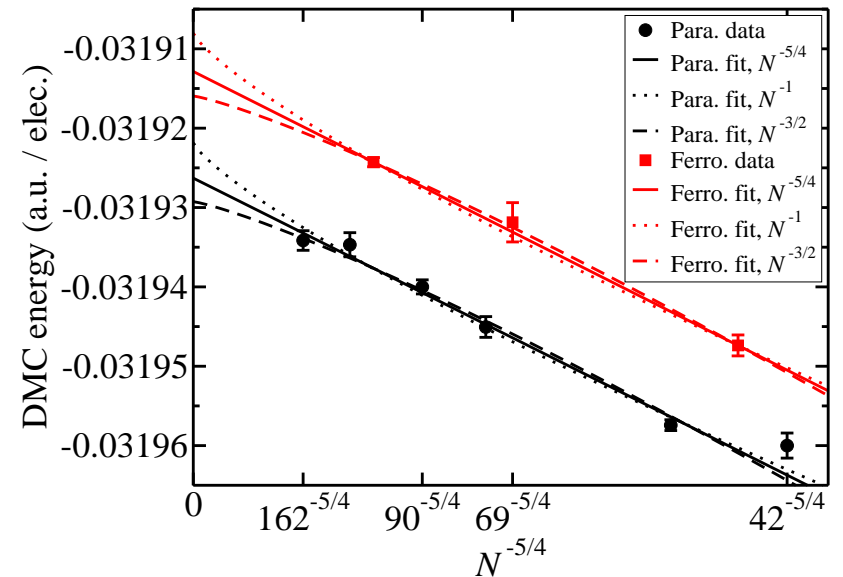
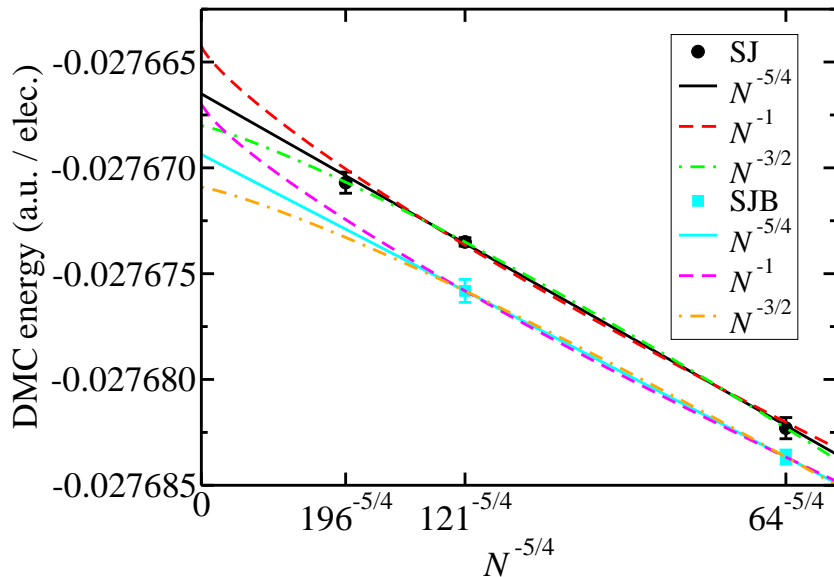
- **Twist averaging in canonical ensemble:** average over all \mathbf{k}_s , keeping N fixed.
 - Replaces grid of \mathbf{k} by a Fermi area (equal to area of Fermi circle), greatly reducing single-particle finite-size effects.
 - Shape isn't quite right: leaves small positive bias in KE.
- Previous QMC studies of 2D HEG have not used twist averaging.

Long-Range Finite-Size Errors

- Compression of XC hole and neglect of long-range two-body correlations in finite cell give error in 2D energy per electron going as $\mathcal{O}(N^{-5/4})$.¹⁴ Extrapolate using:

$$E_N = E_\infty - bN^{-5/4}.$$

- Previous QMC studies have used $N^{-3/2}$ for crystals and N^{-1} for fluid.



Left: crystal extrapolation at $r_s = 35$ a.u.; right: fluid extrapolation at $r_s = 30$ a.u.

¹⁴ N. D. Drummond, R. J. Needs, A. Sorouri and W. M. C. Foulkes, Phys. Rev. B **78**, 125106 (2008).

Backflow Transformation

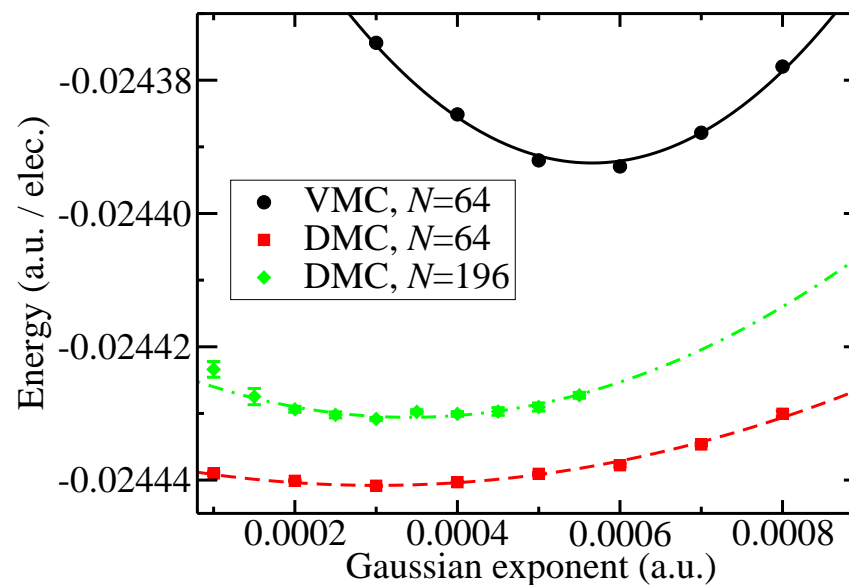
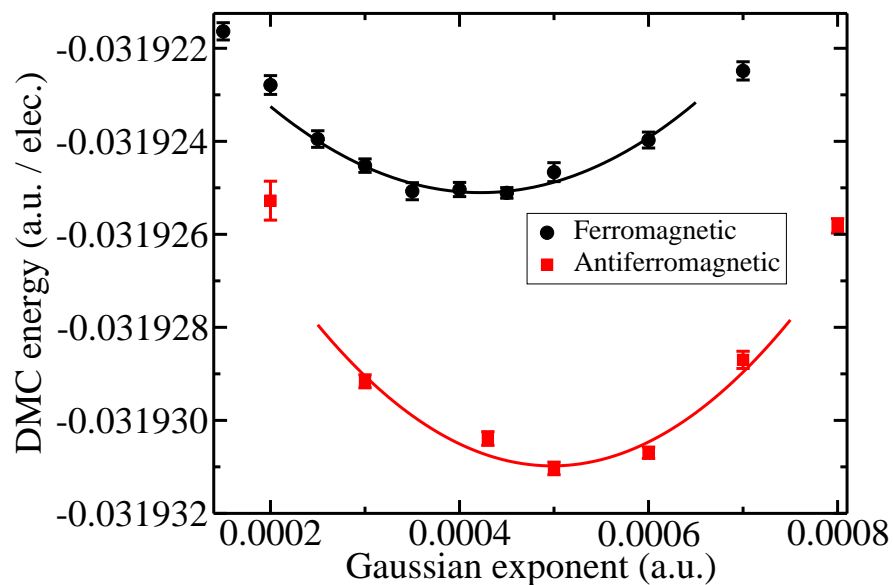
- Evaluate Slater wave function at quasiparticle coordinates related to actual electron coordinates by electron–electron **backflow** functions.¹⁵
- Moves nodal surface of wave function; can improve the fixed-node DMC energy.
- BF is more significant in fluids than crystals, where electrons are already kept apart by localisation on lattice sites.
- Parallel spins are already kept away from each other by wave-function antisymmetry. BF is much less important in ferromagnetic systems.

System ($r_s = 30$ a.u.)	Lowering of DMC energy due to BF ($\mu\text{Ha} / \text{elec.}$)
Paramagnetic fluid	36(3)
Ferromagnetic fluid	6(4)
Antiferromagnetic crystal	2.4(6)
Ferromagnetic crystal	2.3(3)

¹⁵ P. López Ríos, A. Ma, N. D. Drummond, M. D. Towler and R. J. Needs, Phys. Rev. E **74**, 066701 (2006).

Optimisation of Crystal Orbitals (I)

- **Crystal orbitals:** $\phi_{\mathbf{R}}(\mathbf{r}) = \exp(-C|\mathbf{r} - \mathbf{R}|^2)$.
- Only orbital parameter affecting crystal nodal surface: Gaussian exponent C .
 - Minimise DMC energy w.r.t. C to minimise fixed-node error.
 - Then add backflow.

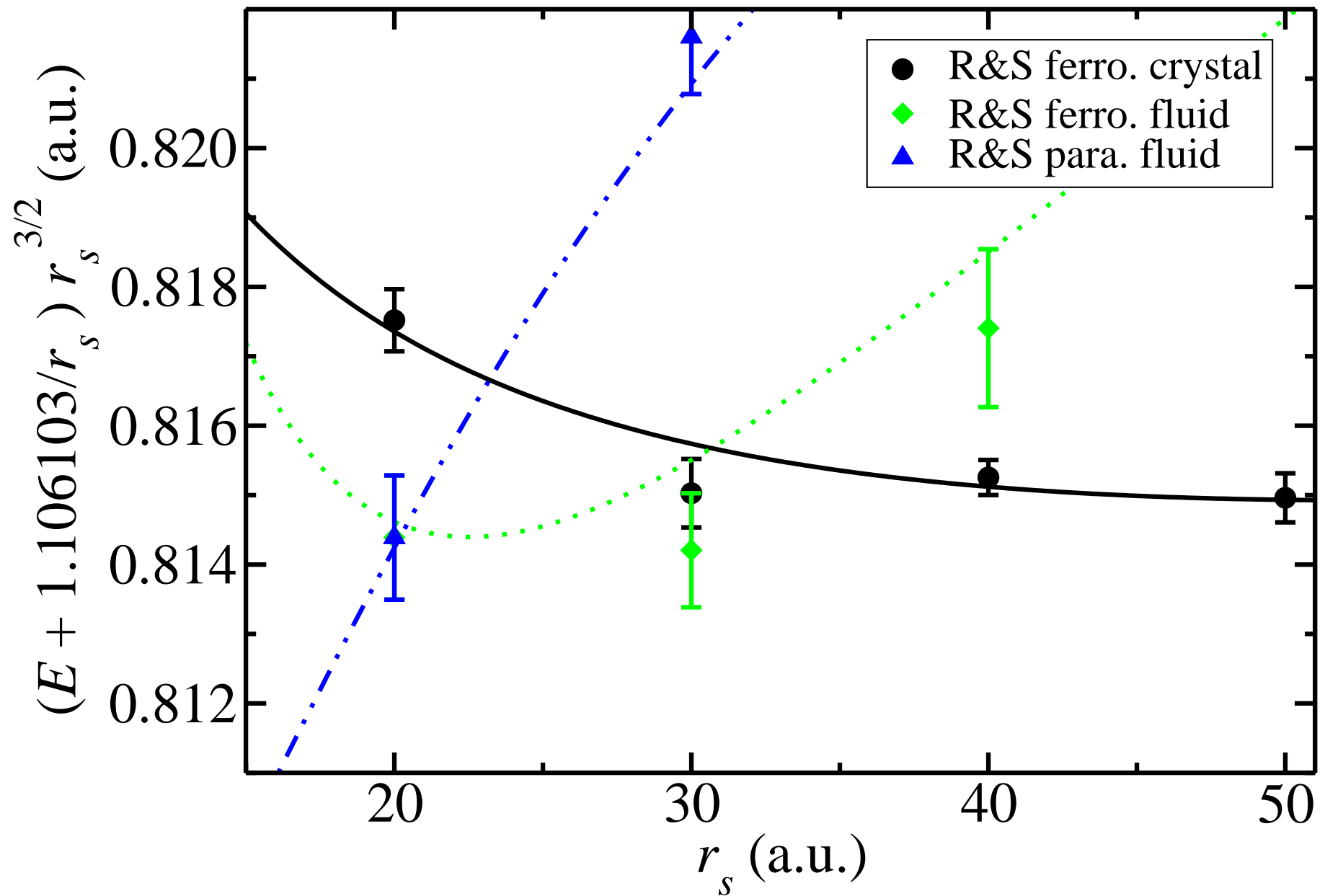


DMC energy against C at $r_s = 30$ a.u. (left) and $r_s = 40$ a.u. (right) (ferro.).

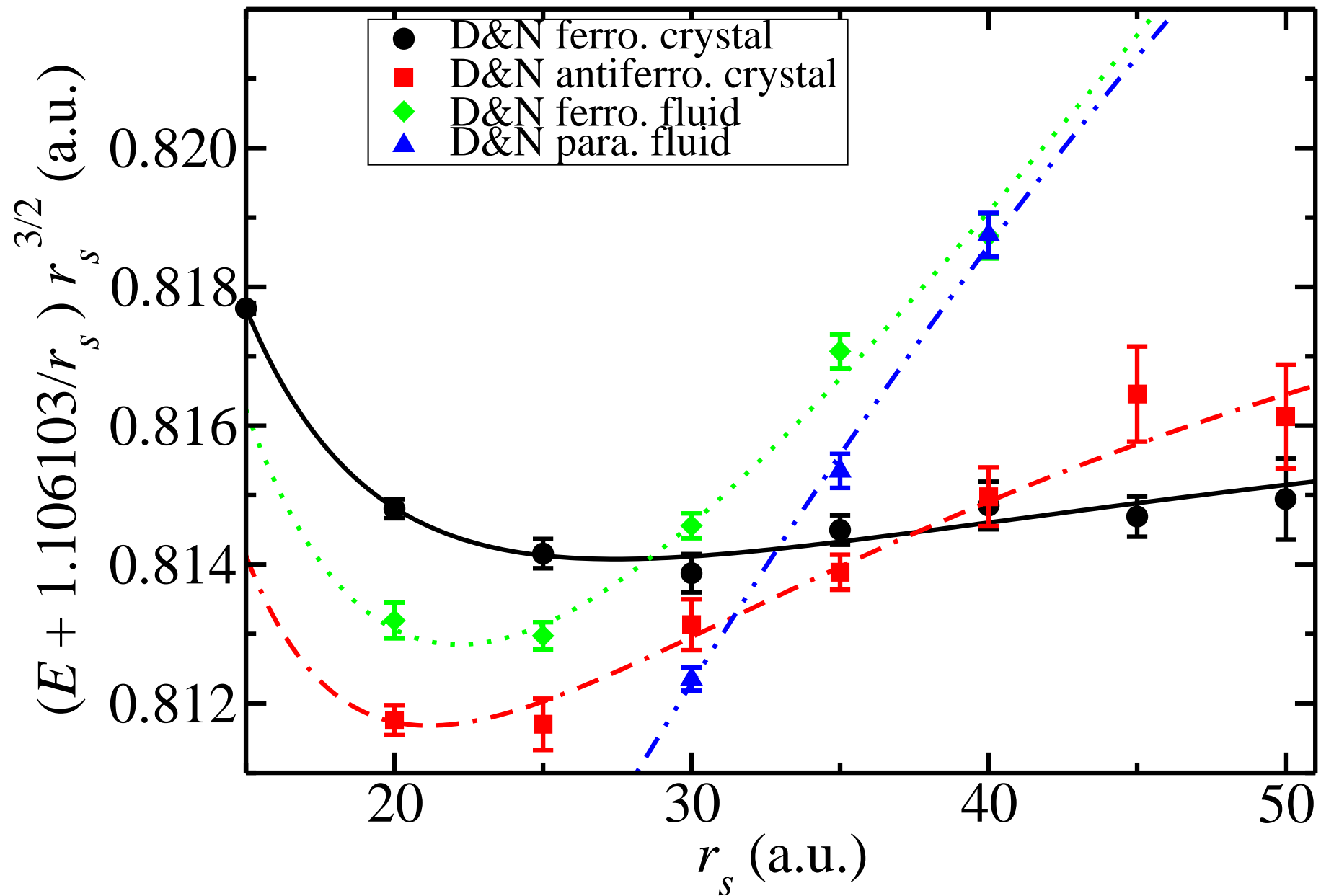
Optimisation of Crystal Orbitals (II)

- **Ferromagnetic crystals:** optimal exponent is $C_{\text{DMC}}^{\text{F}} = 0.071r_s^{-3/2}$.
 - CF, VMC exponent is $C_{\text{VMC}}^{\text{F}} = 0.15r_s^{-3/2}$;
 - HF exponent is $C_{\text{HF}}^{\text{F}} = 0.46r_s^{-3/2}$.
- **Antiferromagnetic crystals:** optimal exponent is $C_{\text{DMC}}^{\text{AF}} = 0.082r_s^{-3/2}$.

2D HEG Energy Diagram (I)



2D HEG Energy Diagram (I)



2D HEG Energy Diagram (II)

- Fully polarised fluid is never stable.
- Wigner crystallisation occurs at $r_s = 31(1)$ a.u. Transition is from a **paramagnetic fluid** to an **antiferromagnetic Wigner crystal**.
- Further transition: **antiferromagnetic** → **ferromagnetic** crystal at $r_s = 38(5)$ a.u.
- At $r_s = 35$ a.u., the energy of a fluid with $\zeta = 2/5$ agrees with the paramagnetic and ferromagnetic fluid energies.
 - Very unlikely that a region of stability for a partially polarised fluid exists.
- Phase transitions in 2D HEG cannot be first order.¹⁶
 - It's energetically favourable to form boundaries between macroscopically separated phases, so a “microemulsion” is formed at crystallisation density.
 - New phases could “round off corners” in energy diagram.

¹⁶ B. Spivak and S. A. Kivelson, Phys. Rev. B **70**, 155114 (2004); R. Jamei *et al.*, Phys. Rev. Lett. **94**, 056805 (2005).

Contact PCF of Paramagnetic Fluid (I)

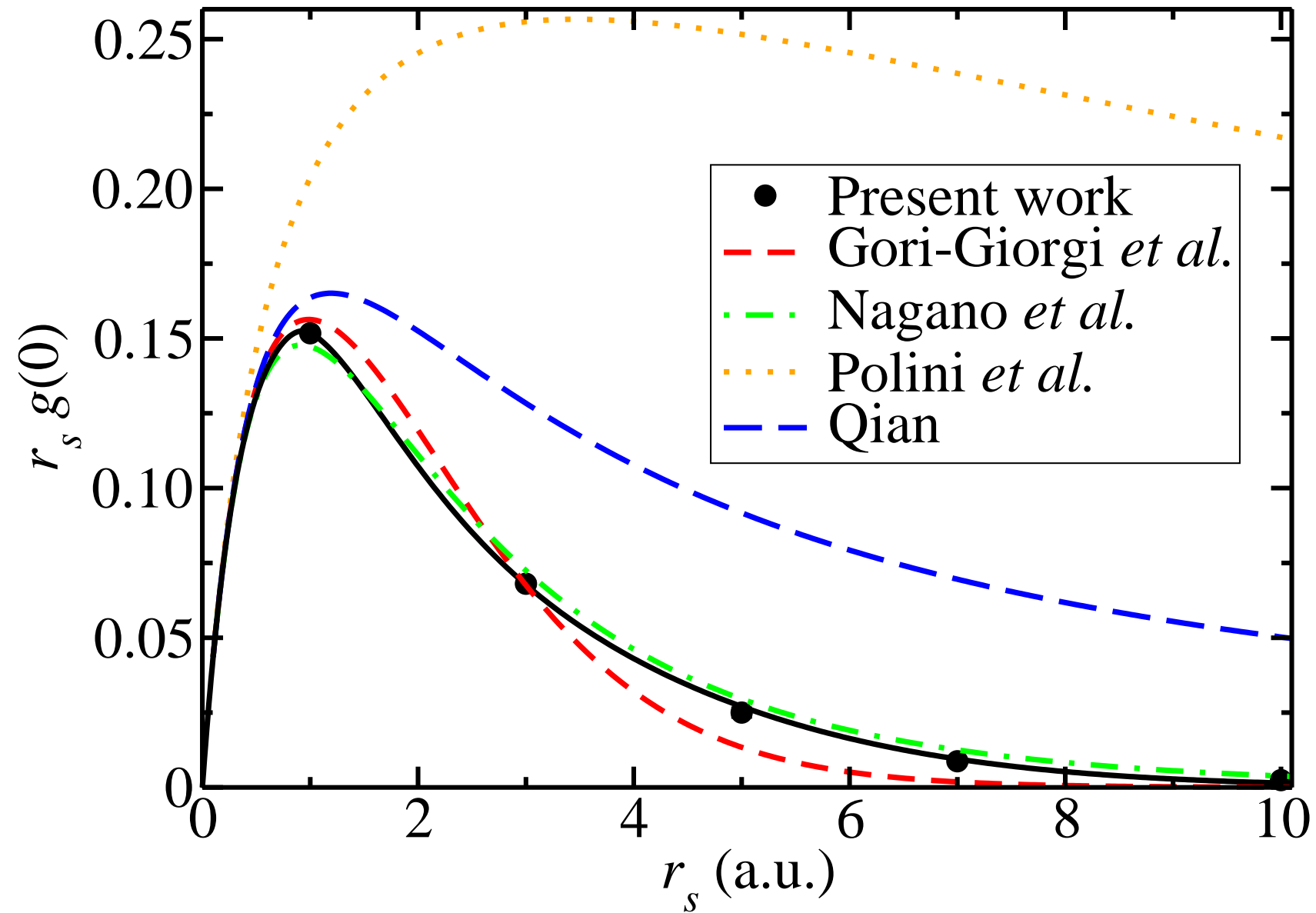
- $g(0)$ is an important parameter in construction of GGA XC functionals for use in DFT.
- Most theoretical calculations of $g(0)$ have used *ladder theory* to solve approximately the Bethe–Goldstone equation for the effective interaction between two electrons. Exact in high-density limit, but not at low densities.
- Disagreement between old approximation¹⁷ in ladder theory and a better approximation,¹⁸ and between the better approximation in ladder theory and QMC.¹⁹
Which is right?
- We evaluate $g(r)$ [including $g(0)$] by binning interparticle distances. Easier in 2D than 3D. Easier at high density than low density.
- Earlier study used Slater–Jastrow wave function and no twist averaging; ours used Slater–Jastrow–**backflow** wave functions and **twist averaging**.

¹⁷ S. Nagano, K. S. Singwi, and S. Ohnishi, Phys. Rev. B **29**, 1209 (1984); *Erratum*, Phys. Rev. B **31**, 3166 (1985).

¹⁸ Z. Qian, Phys. Rev. B **73**, 035106 (2006).

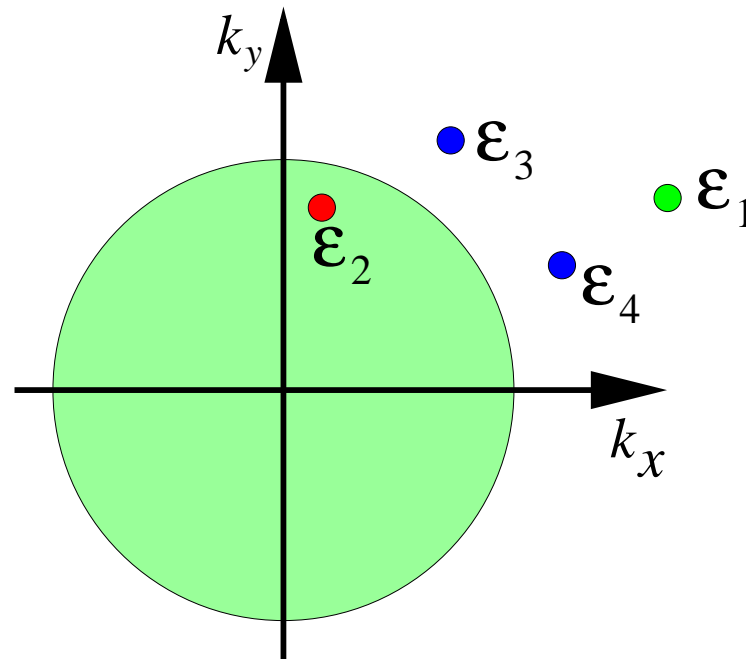
¹⁹ P. Gori-Giorgi, S. Moroni, and G. B. Bachelet, Phys. Rev. B **70**, 115102 (2004).

Contact PCF of Paramagnetic Fluid (II)



Fermi Liquid Theory

- **Fermi liquid theory**²⁰: *low-energy excitations in a fluid of interacting electrons can be treated as excitations of quasiparticles occupying plane-wave states.*
- **Justification**: Pauli exclusion principle. Scattering rate of quasiparticles between plane waves is low (vanishes at Fermi surface). Single-particle momenta are approximately good quantum numbers.



²⁰ L. D. Landau, JETP **3**, 920 (1957); L. D. Landau, JETP **5**, 101 (1957); L. D. Landau, JETP **8**, 70 (1959).

Landau Energy Functional

- Total energy E :

$$E = E_0 + \sum_{\mathbf{k},\sigma} \mathcal{E}_\sigma(\mathbf{k}) \delta N_{\mathbf{k},\sigma} + \frac{1}{2} \sum_{\mathbf{k},\sigma} \sum_{\mathbf{k}',\sigma'} f_{\sigma\sigma'}(\mathbf{k}, \mathbf{k}') \delta N_{\mathbf{k},\sigma} \delta N_{\mathbf{k}',\sigma'},$$

where E_0 is the ground-state energy and $\delta N_{\mathbf{k},\sigma}$ is the change in quasiparticle occupancy relative to the ground state.

- Quasiparticle energy band: $\mathcal{E}_\sigma(\mathbf{k})$ is the energy of an isolated quasiparticle.
 - Linear approximation: near the Fermi surface, $\mathcal{E}_\sigma(\mathbf{k}) = \mathcal{E}_F + (k_F/m^*)(k - k_F)$, where \mathcal{E}_F is the Fermi energy and m^* is the quasiparticle effective mass.
- Landau interaction function: $f_{\sigma\sigma'}(\mathbf{k}, \mathbf{k}')$ describes quasiparticle interactions.
 - Near the Fermi surface, $f_{\sigma\sigma'}$ only depends on the angle $\theta_{\mathbf{k}\mathbf{k}'}$ between \mathbf{k} and \mathbf{k}' .

Quasiparticle Effective Mass of the 2D HEG

- The effective mass (m^*) of a paramagnetic 2D HEG has been the subject of great controversy in recent years:
 - Some experiments²¹ found a large enhancement of m^* at low density; other experiments²² have contradicted this.
 - GW calculations give a range of possible results depending on the choice of effective interaction.²³
 - Previous QMC studies have predicted (i) much less²⁴ and (ii) much more²⁵ enhancement of m^* than found in recent experiments.
- Experiment²² and theory²⁶ suggest that m^* in paramagnetic and ferromagnetic HEGs behaves quite differently as a function of density.

²¹ J. L. Smith and P. J. Stiles, Phys. Rev. Lett. **29**, 102 (1972); V. M. Pudalov *et al.*, Phys. Rev. Lett. **88**, 196404 (2002).

²² Y.-W. Tan *et al.*, Phys. Rev. Lett. **94**, 016405 (2005); M. Padmanabhan *et al.*, Phys. Rev. Lett. **101**, 026402 (2008).

²³ G. F. Giuliani and G. Vignale, *Quantum Theory of the Electron Liquid*, CUP, Cambridge (2005).

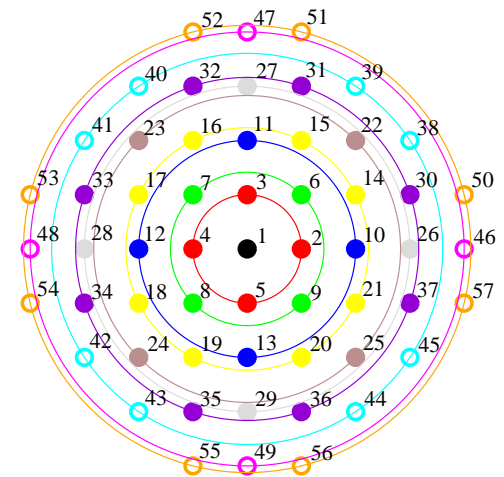
²⁴ Y. Kwon, D. M. Ceperley, and R. M. Martin, Phys. Rev. B **50**, 1684 (1994).

²⁵ M. Holzmann, B. Bernu, V. Olevano and D. M. Ceperley, Phys. Rev. B **79**, 041308(R) (2009).

²⁶ Y. Zhang and S. Das Sarma, Phys. Rev. Lett. **95**, 256603 (2005).

Calculating the Effective Mass and Landau Interaction Functions

- To calculate the quasiparticle effective mass:
 - The DMC energy band $\mathcal{E}(k)$ was determined at a range of k by taking the energy difference when an electron is added to or removed from a closed-shell ground-state.
 - A quartic $\mathcal{E}(k) = \alpha_0 + \alpha_2 k^2 + \alpha_4 k^4$ was fitted to the energy band values.
 - The effective mass was then calculated as $m^* = k_F / (d\mathcal{E}/dk)_{k_F}$.
- To calculate the Landau interaction functions and hence Fermi liquid parameters:
 - Electrons were promoted from (σ, \mathbf{k}) just below the Fermi edge to (σ', \mathbf{k}') just above it, to obtain the energy difference $\Delta E_{\sigma\sigma'}(\mathbf{k}, \mathbf{k}')$ relative to the ground state.
 - The single-particle contribution was subtracted from the excitation energy, to give $-f_{\sigma\sigma'}(\theta_{\mathbf{k}\mathbf{k}'}) = \Delta E_{\sigma\sigma'}(\mathbf{k}, \mathbf{k}') - [\mathcal{E}(\mathbf{k}') - \mathcal{E}(\mathbf{k})]$.
 - The first few Fourier components of $f_{\sigma\sigma'}(\theta)$ were found by numerical integration in order to obtain the *Fermi liquid parameters*.



Fermi Liquid Parameters

- Fermi liquid parameters:

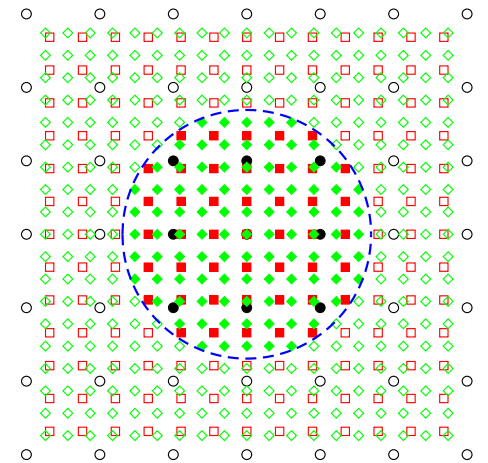
$$F_l^{s,a} = \frac{Am^*}{4\pi^2} \int [f_{\uparrow\uparrow}(\theta_{\mathbf{k}\mathbf{k}'}) \pm f_{\uparrow\downarrow}(\theta_{\mathbf{k}\mathbf{k}'})] \cos(l\theta) d\theta,$$

where $A = \pi r_s^2 N$ is the area of the simulation cell.

- For a ferromagnetic HEG, the Fermi liquid parameters $\{F_l\}$ are given by the expression above with $f_{\uparrow\downarrow} = 0$.
- *We need to obtain a description of the interaction parameters according to a well-defined prescription for energy differences in a finite cell, then extrapolate the Fermi liquid parameters to the thermodynamic limit.*
- Armed with the effective mass and the Fermi liquid parameters, nearly all thermodynamic and transport properties of the fully interacting electron gas can be calculated.

Finite-Size Errors

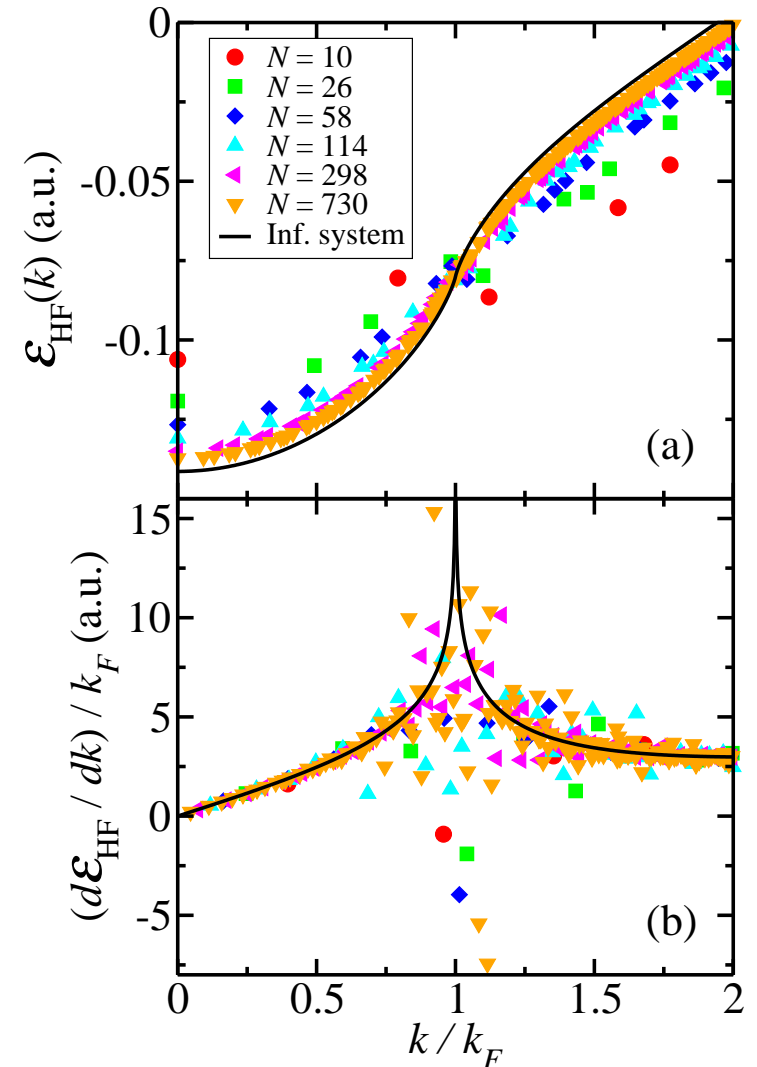
- The calculations were performed in **finite cells** subject to **periodic boundary conditions**.
- **Major source of error and uncertainty in the QMC results:** finite size effects.
- **Momentum quantisation:**
 - In our finite simulation cell subject to (twisted) periodic boundary conditions, the available momentum states fall on the (offset) grid of reciprocal lattice points.
 - This restricts the \mathbf{k} values we can consider.
- **There are also finite size errors in the excitation energies due to the neglect of long-range interactions and correlations in a finite cell.**
 - These errors have been shown to fall off slowly, as $N^{-1/4}$, near the Fermi surface.²⁷



²⁷ M. Holzmann, B. Bernu, V. Olevano and D. M. Ceperley, Phys. Rev. B **79**, 041308(R) (2009).

Pathological Behaviour at the Fermi Surface (I)

- Fermi liquid theory is only valid near the Fermi surface.
- Energy band is defined by Landau energy functional at all \mathbf{k} , but does not correspond to quasiparticle band except near Fermi surface.
- In the infinite-system limit, the exact energy band is smooth and well-behaved everywhere, including the Fermi surface.
- **The Hartree–Fock band is pathological.**
 - In the infinite-system limit it has a logarithmic divergence at the Fermi surface.
 - In finite systems it behaves very badly.



Pathological Behaviour at the Fermi Surface (II)

- *DMC may take you 99% of the way from HF to reality, but this does not get rid of the pathological behaviour from HF theory.*
- Hence we need to consider excitations **away from the Fermi surface** in order to obtain the gradient of the energy band at k_F .
- Finite-size effects in the Fermi liquid parameters are a killer.

Assessing the Accuracy of our DMC Calculations (I)

- **Occupied bandwidth:** $\Delta\mathcal{E} = \mathcal{E}(k_F) - \mathcal{E}(0) = E_-(0) - E_-(k_F)$.
- **DMC BW is expected to be an upper bound:** assuming DMC retrieves the same fraction of the correlation energy in the ground and excited states, the BW will lie between the Hartree-Fock value $E_-^{\text{HF}}(0) - E_-^{\text{HF}}(k_F)$, which is too large, and the exact result $E_-^{\text{exact}}(0) - E_-^{\text{exact}}(k_F)$.
- Likewise, Slater-Jastrow DMC BWs are expected to be greater than Slater-Jastrow-backflow DMC BWs.
- *To obtain an accurate BW, it is essential to retrieve a very large fraction of the correlation energy in the DMC calculations, which explains why the inclusion of backflow is so important.*
- The extent to which the BW is overestimated in HF theory grows with r_s so that, assuming DMC retrieves a constant fraction of the correlation energy, **the DMC bands become less accurate at low density.**

Assessing the Accuracy of our DMC Calculations (II)

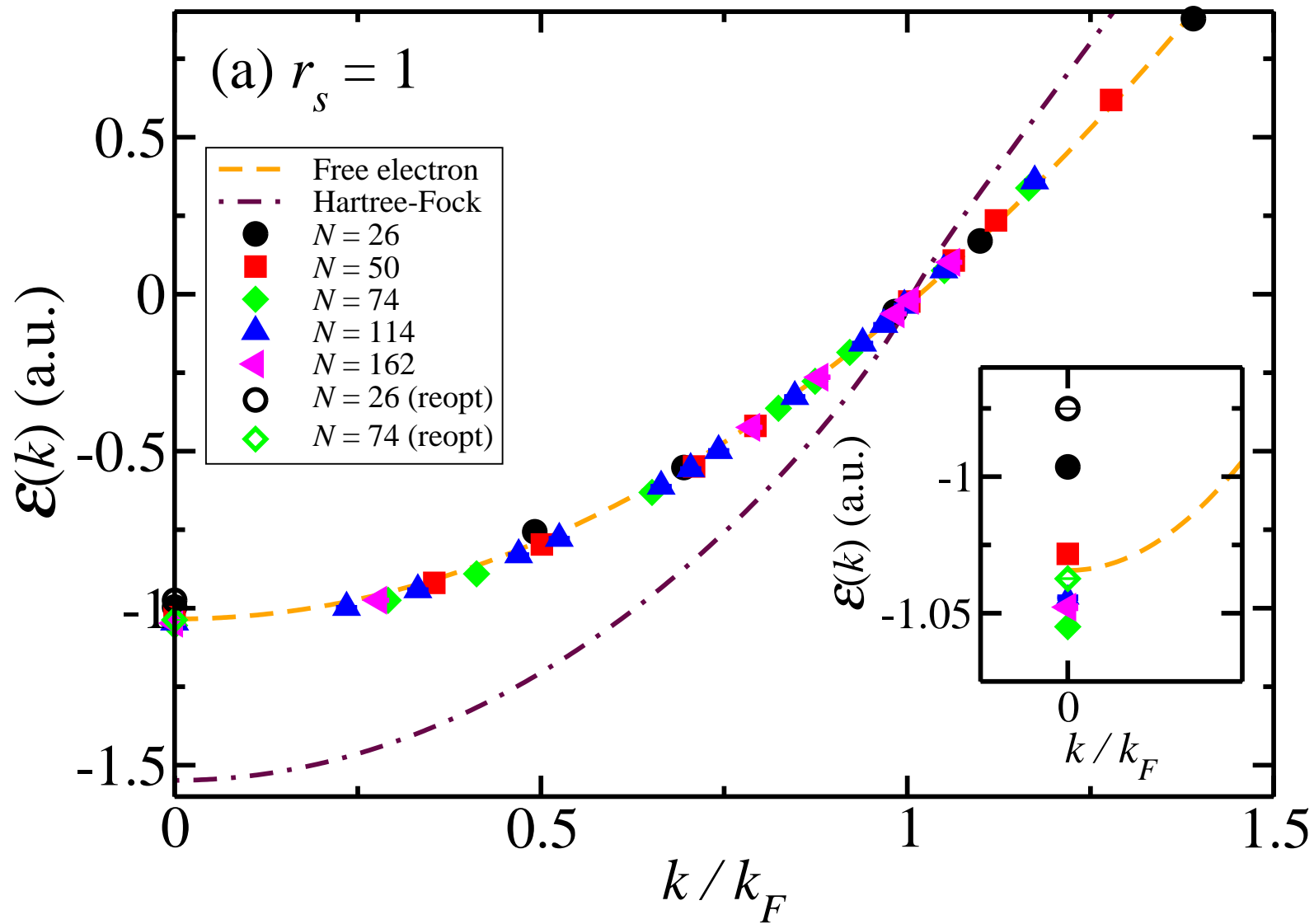
- Extrapolating the VMC energy with different trial wave functions to zero variance suggests that our DMC calculations retrieve more than 99% of the correlation energy, and that the fraction retrieved is similar in both the ground and excited states.
- The free-electron BW is greater than or approximately equal to the exact BW. Hence the error in the HF BW is less than or approximately equal to $\Delta\mathcal{E}^{\text{HF}} - \Delta\mathcal{E}^{\text{free}} = k_F(1 - 2/\pi)$.
- So the error in the DMC BW is less than $0.01k_F(1 - 2/\pi) \approx 0.007/r_s$ for a ferromagnetic HEG and less than about $0.01k_F(1 - 2/\pi) \approx 0.005/r_s$ for a paramagnetic HEG.
 - Since the BW falls off as r_s^{-2} , the error is more significant at large r_s .
 - In the worst case (the paramagnetic HEG at $r_s = 10$) this argument suggests that DMC overestimates the BW by $\sim 9\%$. In the next-worse case (paramagnetic, $r_s = 5$), the BW is overestimated by $\sim 4\%$.
 - It is reasonable to assume that DMC underestimates m^* by a similar amount.

To Reoptimise or Not To Reoptimise

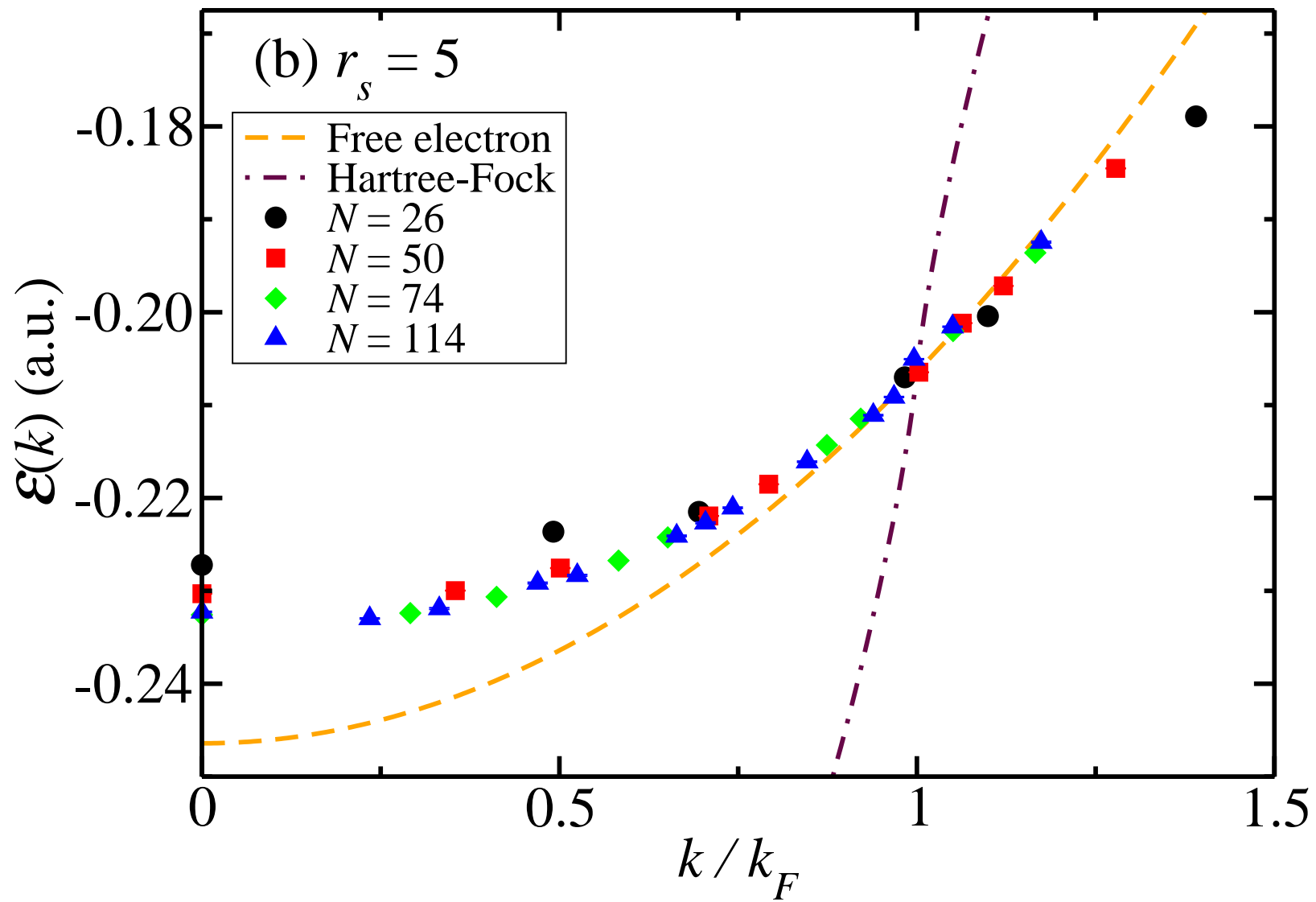
- We optimise the trial wave function in the ground state and then continue to use the same Jastrow factor and backflow function in our excited-state calculations.
- The excitation of a single electron has no effect on the optimal Jastrow factor or backflow function in the thermodynamic limit.
 - Hence the fact that the Jastrow factor and backflow function can be re-optimised in an excited state in a finite cell²⁸ is simply a finite-size effect.
 - More finite-size bias is introduced into the energy band by re-optimising the Jastrow factor and backflow function in each excited state considered.
- It is essential not to re-optimize the wave function when an electron is promoted, to maximise the cancellation of errors that occurs when the single-particle contribution is subtracted out from a difference in total energy.
- Promoting an electron results in smaller finite-size errors than adding two electrons, since the latter modifies the density of the finite system.

²⁸ For example, re-optimising the wave function when an electron is subtracted from $\mathbf{k} = \mathbf{0}$ in a 74-electron HEG at $r_s = 1$ lowers the DMC energy by 0.000241(4) a.u.

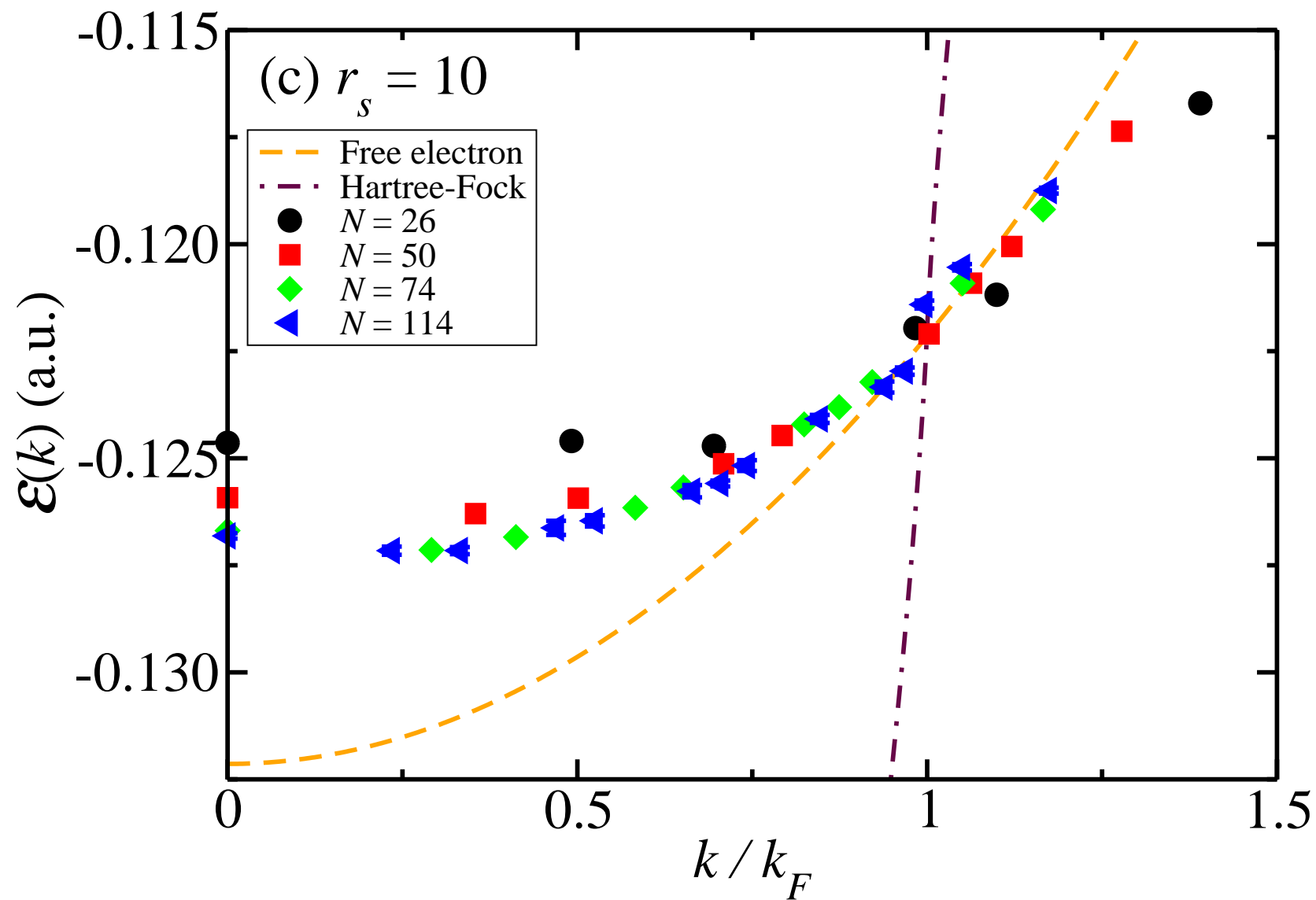
Paramagnetic Single-Particle Energy Band: $r_s = 1$



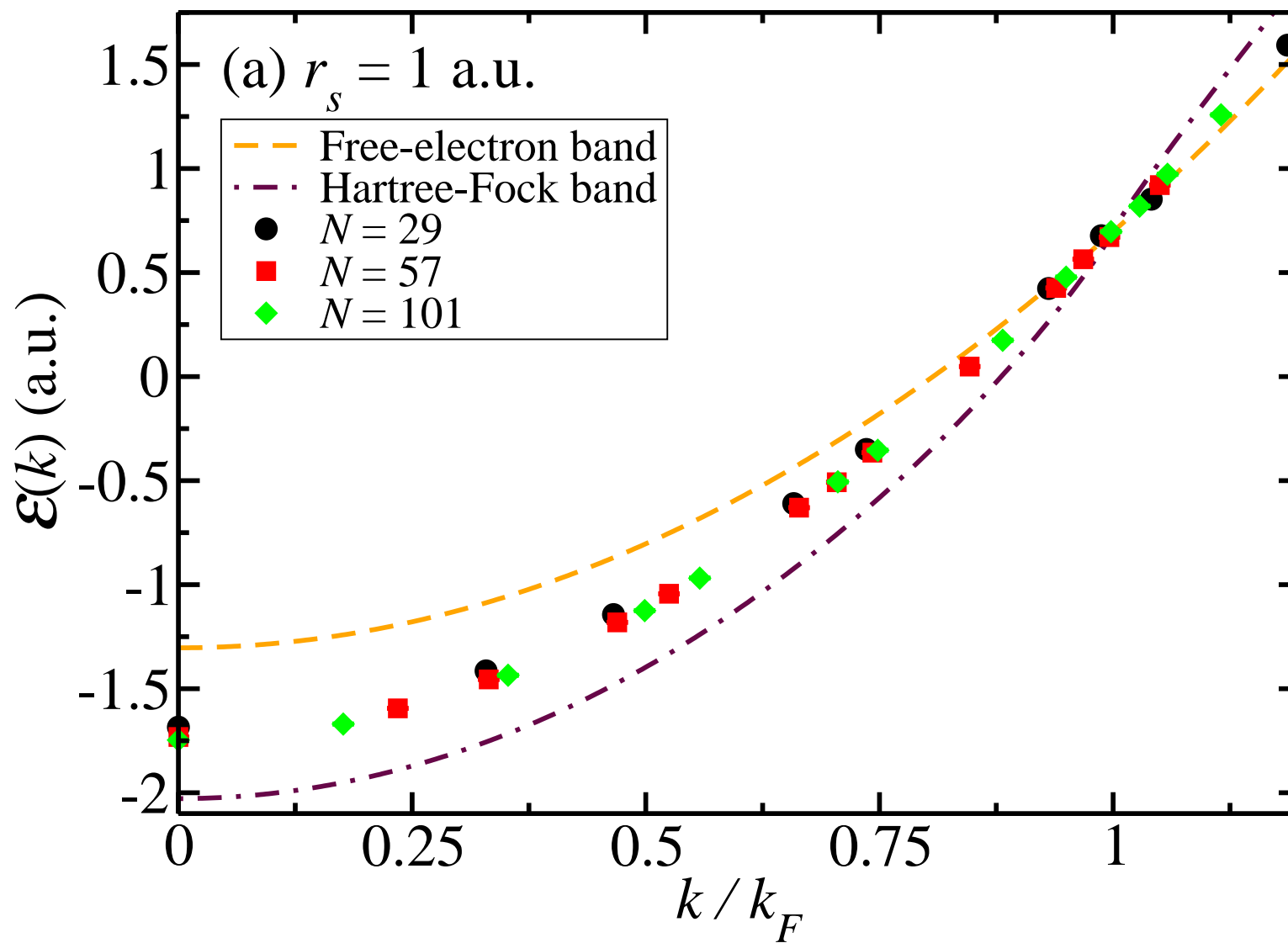
Paramagnetic Single-Particle Energy Band: $r_s = 5$



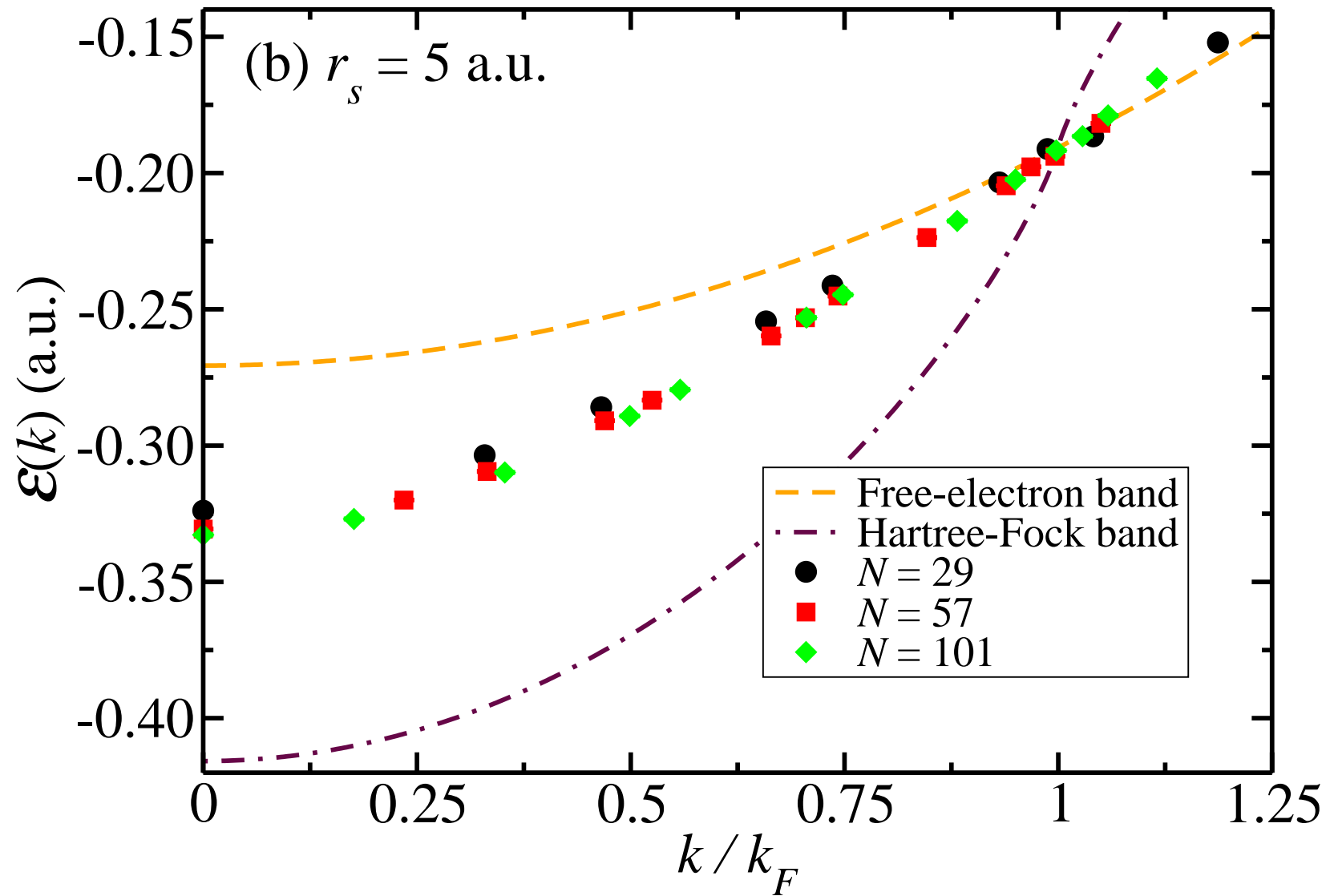
Paramagnetic Single-Particle Energy Band: $r_s = 10$



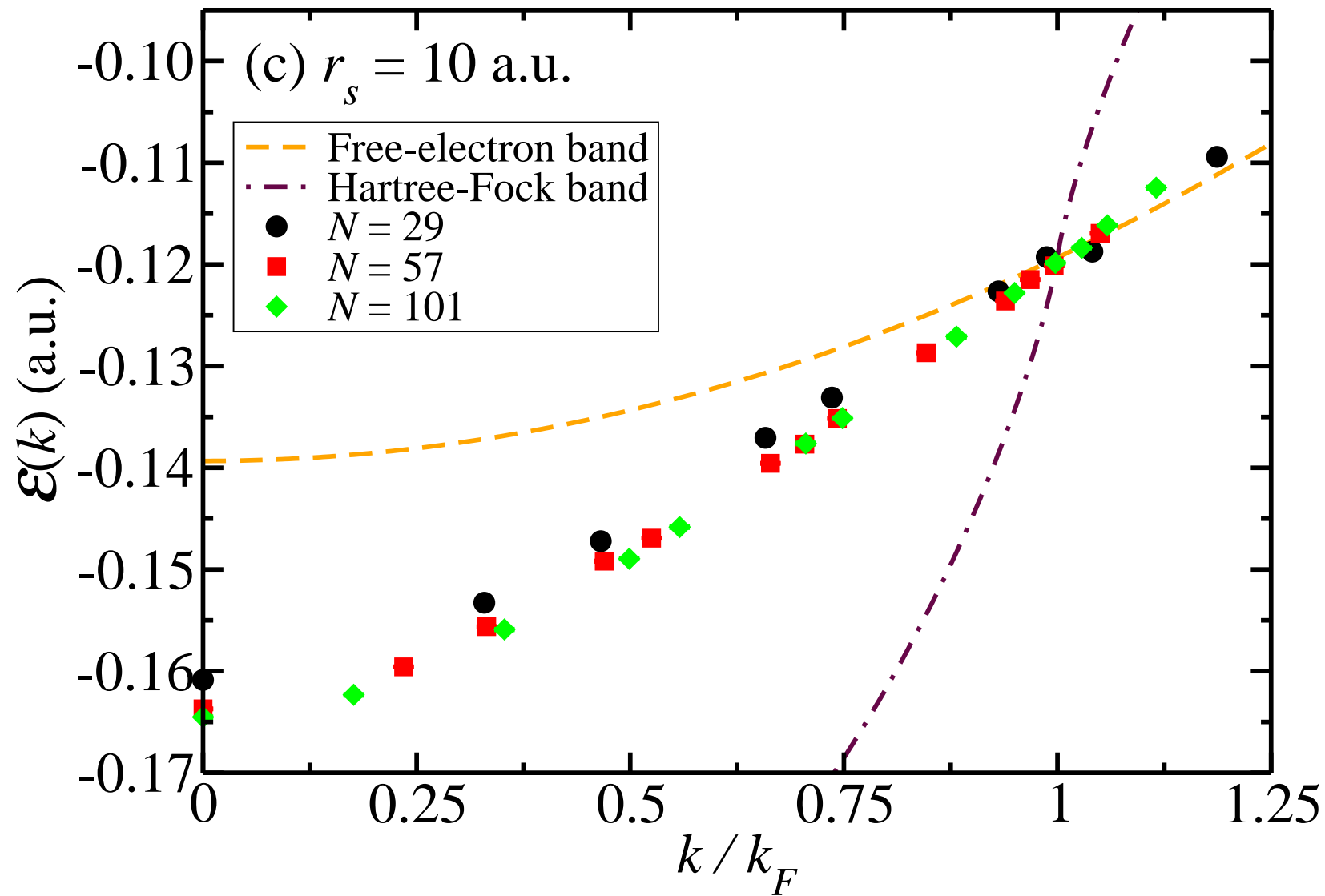
Ferromagnetic Single-Particle Energy Band: $r_s = 1$



Ferromagnetic Single-Particle Energy Band: $r_s = 5$

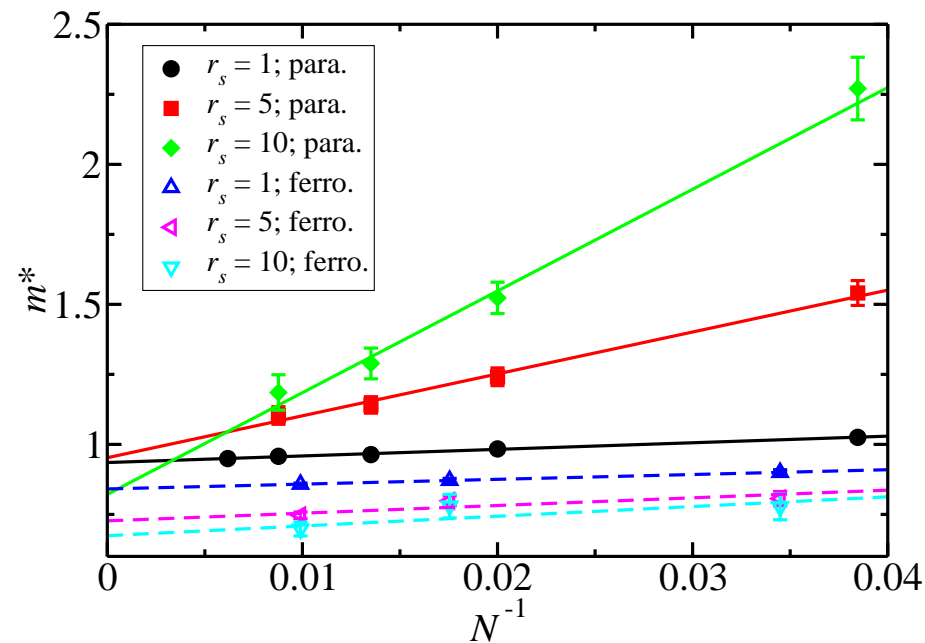


Ferromagnetic Single-Particle Energy Band: $r_s = 10$



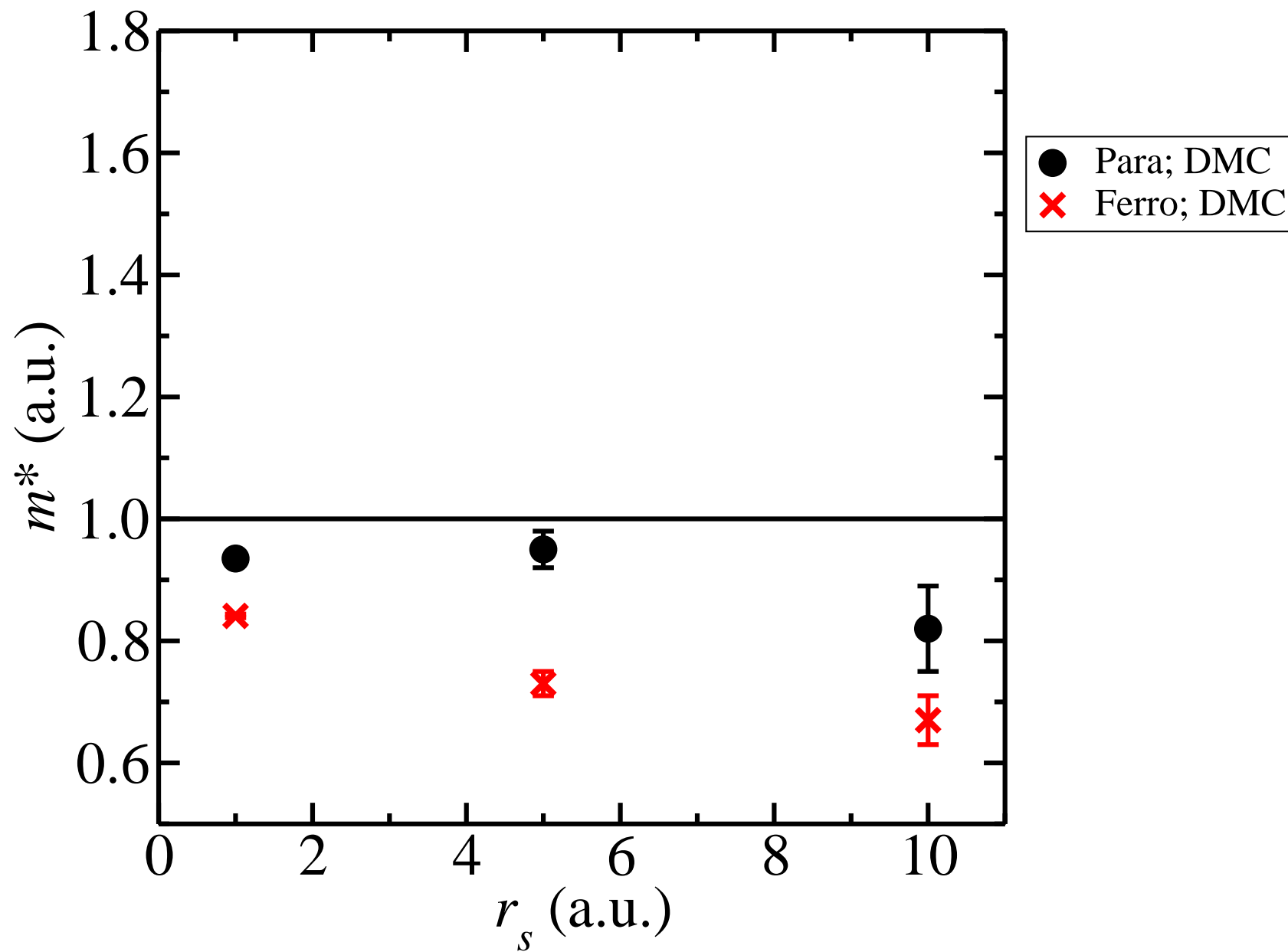
Extrapolation of the Effective Mass to the Thermodynamic Limit

- Effective mass against system size:

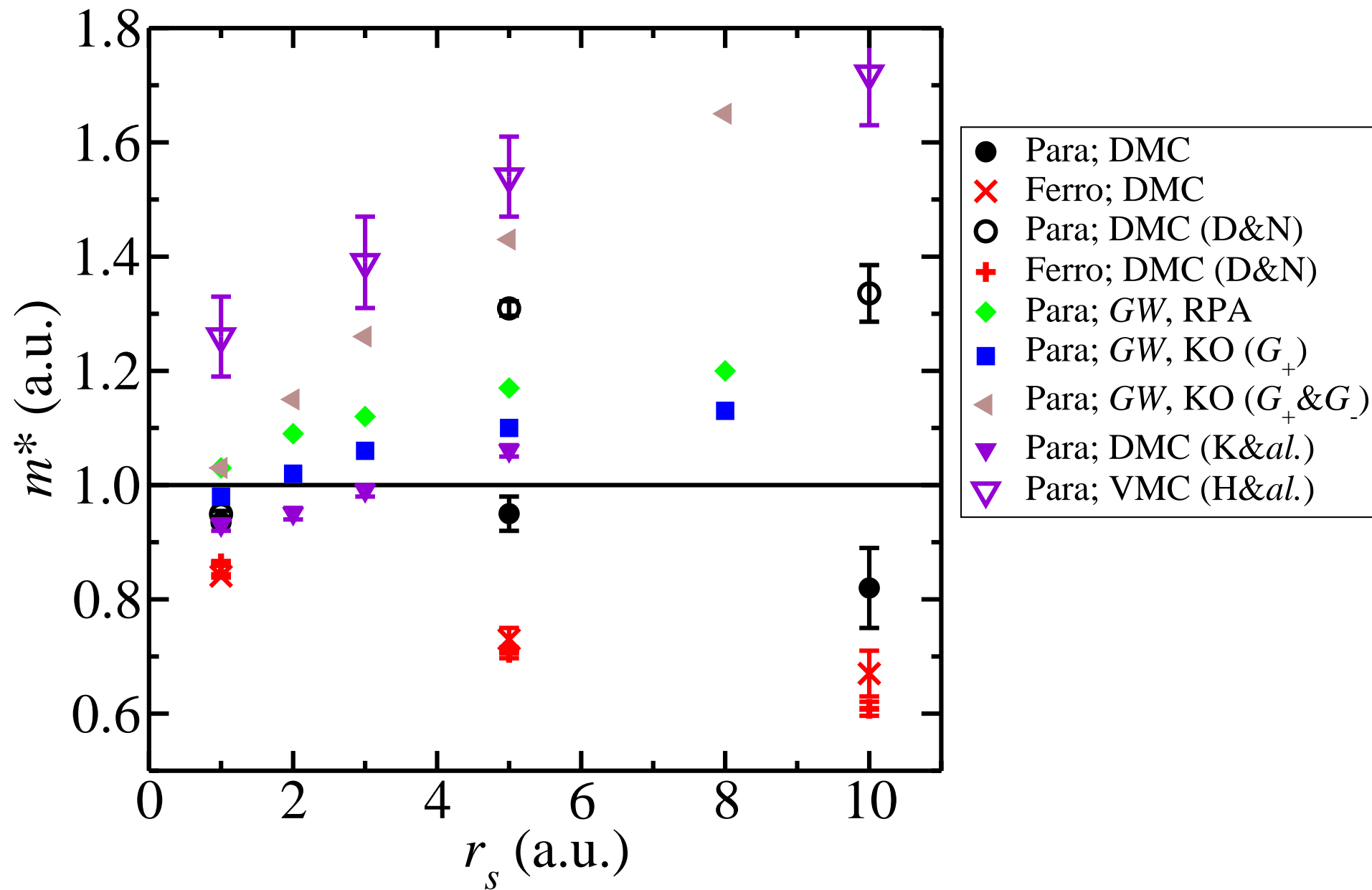


- Scaling is not the $N^{-1/4}$ predicted by Holzmann *et al.* near the Fermi surface, because we have fitted to the entire band.
 - Assume an N^{-1} scaling of the finite-size error.

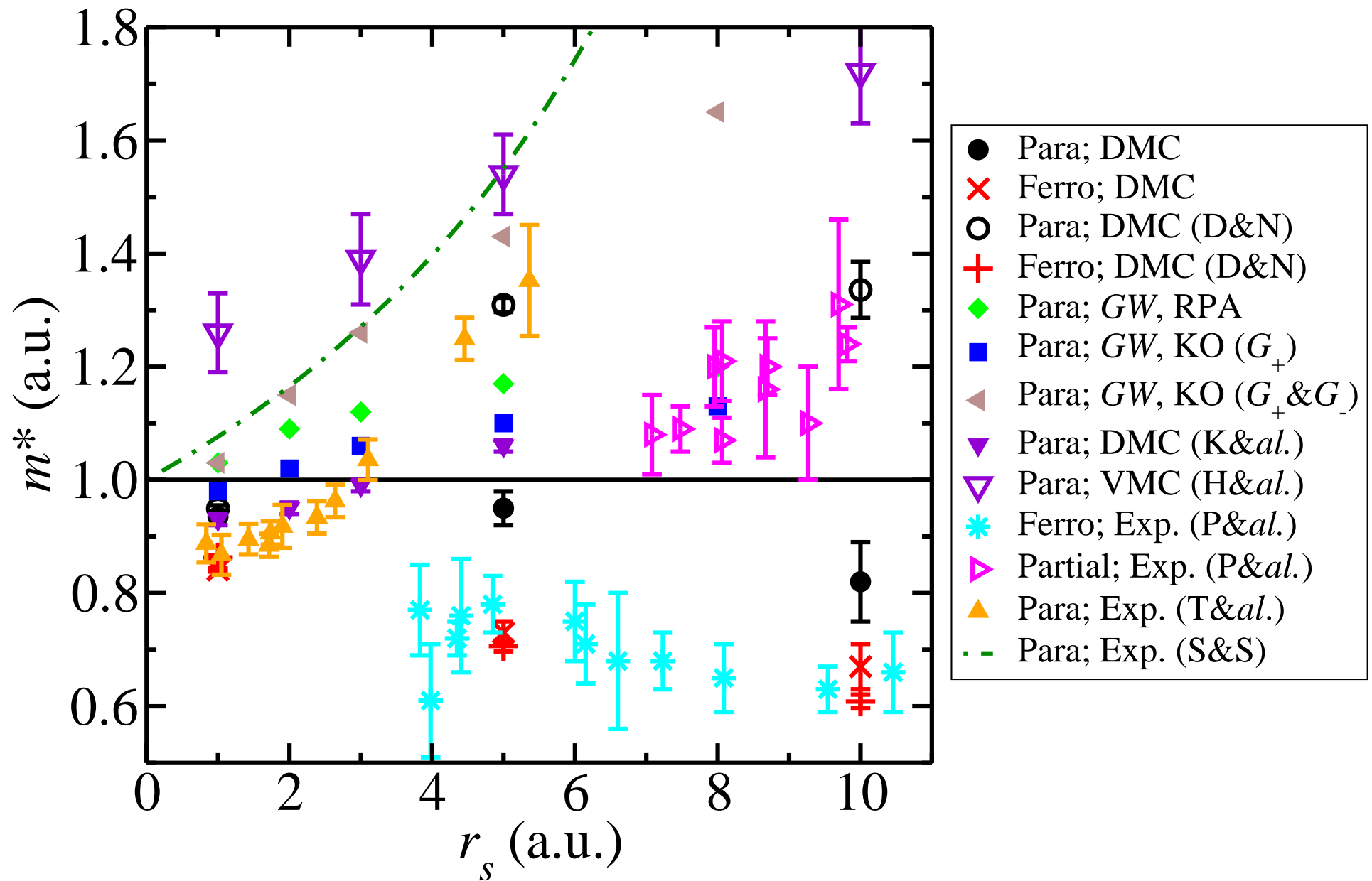
Quasiparticle Effective Masses (I)



Quasiparticle Effective Masses (I)



Quasiparticle Effective Masses (I)



Quasiparticle Effective Masses (II)

- Paramagnetic HEG: effective mass remains close to 1.
- Ferromagnetic HEG: m^* decreases when the density is lowered.
- Our results therefore support the qualitative conclusions of Padmanabhan *et al.*
- Our results suggest that m^* in paramagnetic 2D HEGs does not grow rapidly as the density is reduced.

Conclusions

- *There is no region of stability for a ferromagnetic Fermi fluid in 2D.*
- *Wigner crystallisation occurs at $r_s = 31(1)$ a.u. in 2D. Crystallisation transition is from a paramagnetic fluid to a (frustrated) antiferromagnetic triangular crystal.*
- *Transition from an antiferromagnetic to a ferromagnetic crystal at $r_s = 38(5)$ a.u.*
- QMC results for contact PCF change little when wave function is improved. Suggests they are accurate. Disagreement with recent ladder theory calculation; agreement with old ladder theory calculation.
- Our data show that the quasiparticle effective mass of the ferromagnetic HEG decreases at low density, unlike the paramagnetic HEG.